

LARGE SIGNAL OPERATION OF VARACTOR MULTIPLIERS

763  
by

VAJINDER PAL SINGH

B. S., (Hons. School) Physics, Panjab University, India 1962

M. S., (Hons. School) Physics, Panjab University, India 1963

---

A MASTER'S REPORT

submitted in partial fulfillment of the

requirements for the degree

MASTER OF SCIENCE

Department of Electrical Engineering

KANSAS STATE UNIVERSITY  
Manhattan, Kansas

1967

Approved by:

Robert R. Malik  
Major Professor

LD  
2015  
4  
167  
-565  
2.4

TABLE OF CONTENTS

	Page
INTRODUCTION . . . . .	1
FUNDAMENTAL CONCEPTS . . . . .	2
Langley Rowe Relations . . . . .	2
Varactor Model. . . . .	4
Limitations On operation. . . . .	9
Basic Varactor Multiplier Circuit Configurations. . .	13
Use Of Idlers . . . . .	15
ANALYSIS WITHOUT IDLERS. . . . .	19
ANALYSIS WITH IDLERS . . . . .	39
THE HYPERABRUPT VARACTOR MULTIPLIER. . . . .	53
Efficiency And The Nonlinearity Coefficient . . . . .	53
Multiplier Analysis . . . . .	56
CONCLUSION . . . . .	71
ACKNOWLEDGMENT . . . . .	72
BIBLIOGRAPHY . . . . .	73

## INTRODUCTION

Generation of waves at low and moderate frequencies is no problem with vacuum tube or transistor oscillators. To obtain higher frequencies, the low frequency obtained can be multiplied by making use of the nonlinear characteristics of the tube or transistor, and tuning the output to the appropriate harmonic. For still higher frequencies klystrons or magnetrons are used. But all these devices become inefficient at very high frequencies. Masers are capable of efficiently generating microwave frequencies, but are costly and complicated. New devices such as the Gunn effect oscillator and Read diode are still in the development stages.

Manley and Rowe (4) have suggested a different approach; the possibility of achieving efficient frequency multiplication by use of nonlinear reactance. Since such a device is essentially lossless, high conversion efficiencies are possible. This theoretical model is, to a good approximation, physically realized by the varactor multiplier which is the subject of investigation in this report.

The varactor is a semiconductor diode with a useful nonlinear reverse bias capacitance. It is thus a passive device. The usual practice is to use a low frequency transistor oscillator followed by one or more varactor harmonic multipliers of appropriate orders.

## FUNDAMENTAL CONCEPTS

### Manley-Rowe Relations

Manley and Rowe (4) have derived a set of power conservation relations that are extremely useful in evaluating the performance which can be achieved from a nonlinear reactance device. Only the final results and their interpretations are given here.

First, consider a nonlinear capacitance excited with two angular frequencies  $\omega_0$  and  $\omega_1$ . As a result of the nonlinear capacitance, sidebands with angular frequencies of the form  $m\omega_0 + n\omega_1$ , for positive and negative integral values of  $m$  and  $n$  are generated. As the voltage and current of the capacitor have components at all these sidebands, each can be written in a Fourier series as:

$$v(t) = \sum_{m=-\infty}^{+\infty} \sum_{n=-\infty}^{+\infty} V_{mn} e^{j(m\omega_0 + n\omega_1)t}$$

$$\text{and } i(t) = \sum_{m=-\infty}^{+\infty} \sum_{n=-\infty}^{+\infty} I_{mn} e^{j(m\omega_0 + n\omega_1)t}$$

The time averaged power delivered to the nonlinear capacitor is zero because the capacitor, though nonlinear, is lossless. However, the nonlinearities convert power from one frequency to another.

Let  $P_{mn}$  be the average power input to the capacitor at angular frequency  $m\omega_0 + n\omega_1$ .

Then  $P_{mn} = 2 \operatorname{Re} V_{mn} I_{mn}^*$ , where  $I_{mn}^*$  denotes the complex conjugate in  $I_{mn}$ .

If the capacitor is lossless,

$$\sum_{m,n} P_{mn} = 0, \text{ where this summation extends only over}$$

combinations of  $m$  and  $n$  such that  $m\omega_0 + n\omega_1$  is positive.

The Manley-Rowe formulas provide information in addition to this equation. Not all combinations of  $P_{mn}$  that obey the above equation are possible with non-linear reactances, but only those for which certain weighted sums of the  $P_{mn}$  vanish. The Manley-Rowe formulas are:

$$\sum_{m,n} \frac{mP_{mn}}{m\omega_0 + n\omega_1} = 0$$

$$\sum_{m,n} \frac{nP_{mn}}{m\omega_0 + n\omega_1} = 0$$

Multiplying the first equation by  $\omega_0$  and the second by  $\omega_1$ , and then adding one obtains  $\sum_{m,n} P_{mn} = 0$

Thus the two Manley-Rowe formulas imply that the capacitor is lossless, and together constitute one relation in addition to the condition of losslessness.

The discussion up to this point has been general. Now, in the particular case of a harmonic multiplier where only one driving frequency is used, one obtains the appropriate Manley-Rowe formula by setting  $m = 0$ . Thus if  $P_n$  is defined as the

average power input at angular frequency  $n\omega_1$ , then

$$\sum_{n=1}^{\infty} P_n = 0$$

It should be noted that this equation is slightly different from the condition of losslessness, as here the dc power is excluded. The Manley-Rowe formula thus predicts that the output at any harmonic cannot be increased by supplying dc power. The Manley-Rowe conditions are general power conservation relations and do not depend on any specific circuit.

#### Varactor Model

In order to arrive at the mathematical expressions characterizing the performance of the varactor, it is necessary to represent the varactor by an equivalent circuit. At first the complete model will be given and the various parameters will be discussed. Their relative importance will then allow one to make suitable approximations to arrive at the final simplified model.

Figure (1a) gives the complete equivalent circuit of the diode.

The depletion layer capacitance,  $C(V)$ , is of primary importance when the diode is used as a varactor. Its physical source may be visualized as follows. The electric field inside the junction of a reverse biased diode is always in a direction such that it sweeps electrons towards the n-side and holes towards the p-side. This leaves a region with very few mobile carriers so that the excess donor

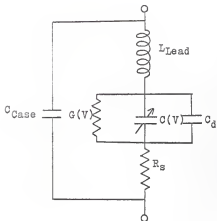


Figure 1a. Complete equivalent circuit of varactor.



Figure 1b. Simplified varactor equivalent circuit.

and acceptor ions are uncompensated. This region with stationary charges, called the depletion layer, is equivalent to a parallel plate condenser with spacing between the plates equal to the width of the depletion region. From Fig. (2a) it is clear that the width of this region, hence the capacitance, will vary with applied voltage. When the applied voltage is zero, the junction has an electric potential  $V_\phi$  across it, and the depletion layer has some finite width. For forward voltages, the depletion layer becomes thinner, and finally when  $V = V_\phi$ , it vanishes. Thus in the limit as  $V$  approaches  $V_\phi$ , the depletion layer capacitance approaches infinity.

The equation that describes the depletion layer capacitance-voltage relationship is given by:

$$C(V) = \frac{C_0}{\left(1 - \frac{V}{V_\phi}\right)^m}$$

where  $C_0$  is the capacitance at zero bias,

$V_\phi$  is the contact potential,

$V$  is the voltage across the varactor, and

$m$  is a constant which depends on doping. It is one half for abrupt junctions and one third for graded junctions.

The  $C - V$  curve is shown in Fig. (2b).

The diffusion capacitance, which arises when a diode is forward biased, is accounted for by  $C_d$ . It is associated with the storage of minority carriers, or the redistribution



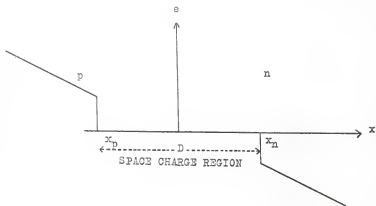


Figure 2a. A typical impurity and mobile charge distribution across a p-n junction.

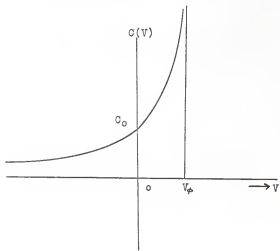


Figure 2b. Nonlinear capacitance arising due to depletion layer capacitance.

of the minority carriers, when the diode is injecting such carriers due to its bias condition. Its effect is that of a capacitance in parallel with the depletion layer capacitance.

The parasitic series resistance,  $R_s$ , is the second most important parameter of the varactor diode. Physically,  $R_s$  includes the bulk resistance of the semiconductor and the resistance of the leads. The bulk resistance component of  $R_s$  includes only the region outside the depletion layer. Thus the series resistance depends on the depletion layer thickness. As the capacitance increases, the series resistance also increases.

It is clear from the discussion above that  $R_s$  is voltage dependent and itself can lead to frequency conversion. However, for most present day varactors the variation in  $R_s$  with applied voltage is small, therefore  $R_s$  is assumed to be constant. It should be pointed out that  $R_s$  is distinct from and ordinarily much greater than the series resistance that predominates at high forward currents.

The conductance  $G(V)$  accounts for the leakage of current between the terminals of the varactor, both over the surface of the semiconductor and along the package.

As the symbols indicate,  $L_{Lead}$  represents the inductance of wires leading to the semiconductor, and  $C_{Case}$  represents the stray capacitance of the package enclosing the varactor.

The complete equivalent circuit as shown in Fig. (1a) can be reduced to a simpler form making some approximations.

The effect of the diffusion capacitance can be ignored because its contribution to the total capacitance is important only when the voltage becomes positive, and hence is small. At very high frequencies, in good quality varactors,  $G(V)$  is effectively shunted by  $C(V)$  and hence may be neglected. Also  $L_{Lead}$  and  $C_{Case}$  are neglected for two reasons: first, they are negligible in value; second, their presence does not fundamentally degrade the achievable performance of the varactor, although it may make these derived limits harder to attain.

Neglecting  $G(V)$ ,  $C_{Case}$ ,  $L_{Lead}$ ,  $C_d$  and taking  $R_s$  to be constant, one obtains the simplified equivalent circuit as shown in Fig. (1b). From this model it is seen that one has a nonlinear capacitance available which can be used for frequency multiplication. However, because of the series resistance, it is not lossless like the ideal Manley-Rowe model, and hence does not obey their relations strictly.

Having shown that a non-linear capacitance can be obtained, it may be pointed out that in order to effectively use the nonlinearity of the  $C - V$  curve, large signal operation is desirable. Therefore, the following analysis will be from a large signal point of view.

#### Limitations On Operation

In order to understand the practical limitations on the magnitude of applied voltage, the motion of charges in the varactor under applied voltage is considered.

The hole and electron concentrations near a p - n junction under various bias conditions are shown in Figs. 3(b) to (e). The maximum reverse bias that can be applied is the breakdown voltage  $V_R$ , because there the junction starts conducting copiously as a result of the avalanche multiplication process. Now when a forward bias voltage is applied, the carriers cross the junction and intermingle with the oppositely charged carriers. It is the subsequent neutralization which leads to the forward biased current.

The equation valid for reverse and slightly forward bias voltage is:

$$I = I_S (e^{qV/KT} - 1),$$

where  $I_S$  is the reverse saturation current,  $q$  is the electron charge,  $K$  the Boltzmann constant and  $T$  is the absolute temperature.

As the forward junction voltage approaches  $V_\phi$  the current becomes very large, in fact it is limited only by the dc resistance of the semiconductor material. This voltage is therefore a fundamental limitation on the forward applied dc voltage. Usually the saturation current is quite small and the magnitude of the forward current is not significant until the voltage gets close to  $V_\phi$ . Therefore the varactor can be driven over the range  $V_R \ll V \ll V_\phi$ . For most varactors  $V_\phi$  is about one volt.

Now consider what happens when a signal of very high frequency is applied. During the positive half of the cycle

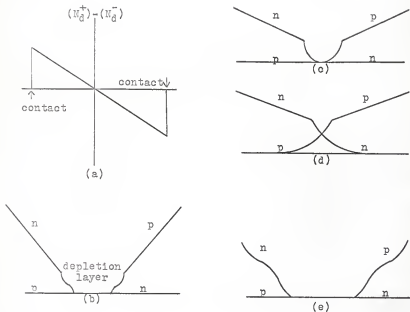


Figure 3a. Impurity distribution in linearly graded junction.

(b) to (e) Hole and electron concentrations in the neighborhood of a graded p-n junction.  
 (b) Zero bias (c) Small forward bias (d) Large forward bias (e) Reverse bias

the mobile charge carriers (holes or electrons) cross the junction as shown in Fig. (3d) and intermingle. However, these migrated carriers have a certain lifetime before they recombine. If the applied voltage is reversed before the carriers have a chance to recombine, most of the carriers will be drawn back across the junction and very few will have recombined. The dc current is made up only from those that do recombine; thus the rectification mechanism fails when the period of applied voltage is considerably below the lifetime. In a varactor diode, the minority carriers have a lifetime,  $\tau$ , in the range  $10^{-6}$  to  $10^{-3}$  sec; and the signal frequencies are usually of the order of  $10^9$  Hz; thus the period is of the order of  $10^{-9}$  sec. Therefore the forward voltage need not be limited to  $V_{\phi}$ , but instead can be somewhat higher. There is experimental evidence that driving the diode into the forward region beyond  $V_{\phi}$  results in higher conversion efficiency (5). However, since no mathematical model is available for describing this effect, operation between  $V_R$  and  $V_{\phi}$  is assumed.

#### Figure Of Merit

A practical upper limit on the frequency of the applied voltage is given by the cut off frequency defined by:

$$f^c = \frac{1}{2\pi R_S C_m}$$

where  $C_m$  is the minimum depletion layer capacitance, that is, the capacitance for reverse voltage just short of  $V_R$ .

Clearly, the cut off frequency is a measure of the highest frequency at which the diode behaves primarily as a capacitance. At higher frequencies, the diode appears primarily resistive.

#### Basic Varactor Multiplier Circuit Configurations

Two of the basic circuits employed for frequency multiplication are shown in Figs. (4) and (5). The names of the two types are associated with the manner in which the diode is imbedded with respect to the input and output circuits. The circuit of Fig. (4) is known as a series type multiplier, because the diode is in series with the source at the angular frequency  $\omega$  and with the load at angular frequency  $N\omega$ . The generator admittance is represented by  $Y_g$ , and  $Y_L$  is the load admittance. The load is usually a pure conductance. The ideal filters  $F_1$  and  $F_N$  are designed such that they are short circuits at all angular frequencies except  $\omega$  and  $N\omega$  respectively. The diode voltage is constrained by the filters to have sinusoidal components only at angular frequencies  $\omega$  and  $N\omega$ . The appropriate coefficients of the two voltage components are first evaluated. Then the  $Q - V$  relationship for the diode is expressed as:

$$Q = Q(V)$$

where  $Q$  is the charge expressed in terms of the voltage  $V$ . This enables the fundamental and the  $N$ th. harmonic charges and hence the corresponding currents to be obtained in terms of  $V_1$ , the fundamental voltage.

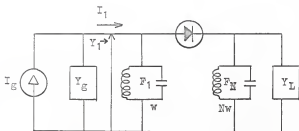


Figure 4. A series type multiplier circuit.

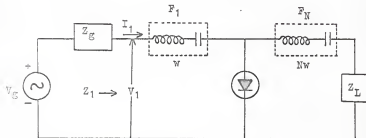


Figure 5. A parallel type multiplier circuit.



The circuit of Fig. (5) is called the parallel type multiplier. Here  $Z_G$  is the source impedance. The ideal filters  $F_1$  and  $F_N$  are now open circuits at all angular frequencies except at  $\omega$  and  $N\omega$  respectively. The method of solution is similar to the series type. Here one chooses to specify charge rather than voltage as the independent variable. Starting with a charge waveform of prescribed harmonic content, one can solve for the terminal voltage of the varactor. In this case the  $Q - V$  relationship is expressed in the form:

$$V = V(Q),$$

and solutions are obtained for  $V_1$  and  $V_N$  in terms of the fundamental charge.

#### Use Of Idlers

Sometimes it is necessary to modify the basic multiplier circuits through the addition of idler circuits. An idler circuit is an additional circuit resonant at the  $m$ th. harmonic such that  $1 < m < N$ . In a parallel multiplier circuit this would imply that currents at three frequencies, the fundamental, the  $m$ th. harmonic and  $N$ th. harmonic can flow through the diode. A parallel type multiplier with an idler circuit is shown in Fig. (6).

The use of idlers is easily understood from the following example. Consider the case of the abrupt junction varactor imbedded in a parallel-type multiplier circuit. For the diode:

$$\frac{Q}{V} = \frac{K}{V^2}$$

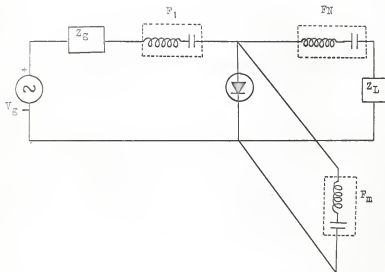


Figure 6. A parallel type idler multiplier with an idler circuit.

Therefore

$$V = \frac{1}{K_a} Q^2$$

Thus the diode is a square law device over its entire range because the voltage is proportional to the square of the charge. Let the diode input current at angular frequency  $\omega_1$  be :

$$I_{in} = I e^{j\omega_1 t} + I^* e^{-j\omega_1 t}$$

Therefore

$$\begin{aligned} Q &= \frac{I}{j\omega_1} e^{j\omega_1 t} + \frac{I^*}{-j\omega_1} e^{-j\omega_1 t} \\ &= Q_1 e^{j\omega_1 t} + Q_1^* e^{-j\omega_1 t} \end{aligned}$$

The diode voltage developed will then be:

$$V = \frac{1}{K_a} Q^2 = \frac{1}{K_a} (Q_1^2 e^{j2\omega_1 t} + Q_1^* e^{-j2\omega_1 t} + 2Q_1 Q_1^*)$$

It is thus seen that there is no voltage developed for harmonics higher than the second. However, such a diode can be used to obtain the third harmonic with the introduction for an idler circuit as shown in Fig. (6), where  $F_M$  and  $F_N$  are now filters that are short circuits for angular frequencies  $2\omega_1$  and  $3\omega_1$  respectively. Current at  $\omega_1$  flows in the input circuit and current at  $2\omega_1$  flows in the idler circuit. These two components mix while flowing through the diode to give the  $3\omega_1$  component, which is then constrained

to flow through the output circuit.

The idler circuit was indispensable in the above case where an abrupt junction varactor must be used to obtain harmonics higher than the second. With a graded junction varactor, the second or third harmonic can be obtained directly without use of idler circuit. However, even in such cases, introduction of the idler circuit helps to improve the efficiency and power output.

The idler circuit should be resonant at such a frequency that the output frequency is related to the input and idler frequency in one of the following manners.

1. Sum of these two frequencies.
2. Difference of these two frequencies.
3. Twice one of these frequencies.

This shows that an abrupt junction diode can be used as a three times or four times multiplier by including an idler at  $2\omega_1$ . To get higher multiplication, more than one idler circuit is required.

## ANALYSIS WITHOUT IDLERS

A varactor multiplier without idlers will now be analyzed. The equivalent circuit of the varactor is represented by Fig. (1b). The complete equivalent circuit of the multiplier to be analyzed is shown in Fig. (7). Filters  $F_1$  and  $F_N$  are such that only current at the fundamental frequency  $\omega$  can flow in the input circuit, and that only current at frequency  $N\omega$  can flow in the output circuit.  $L_1$  and  $L_N$  are tuning inductances for the fundamental and output frequencies, respectively.

Such a circuit has been analyzed by Scanlan and Laybourn (7). Their method is summarized as follows. The voltage across the varactor is expressed as a Fourier series in the harmonic charges. Then, by viewing the input circuit as a source of angular frequency  $\omega$  in series with an impedance, and the output circuit as a voltage generator of angular frequency  $N\omega$  in series with an impedance, the relevant coefficients of the series are found. After a suitable phase evaluation, an expression for efficiency is found which can then be optimized with respect to the various parameters.

The depletion layer capacitance  $C(V)$  is given in terms of the voltage across the junction by:

$$C(V) = \frac{C_0}{\left(1 - \frac{V}{V_0}\right)^m} \quad (1)$$

where  $C_0$  is the zero-bias capacitance and  $V_0$  is the built-in potential.

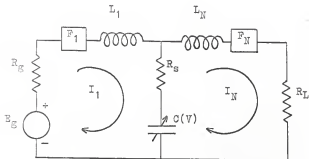


Figure 7. Equivalent circuit of multiplier.

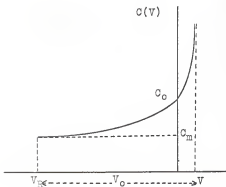


Figure 8. Capacitance versus voltage curve.

At reverse breakdown voltage  $V_R$ ,

$$C(V) = C_m = \frac{C_0}{\left(1 - \frac{V}{V_\phi}\right)^m} \quad (2)$$

Substituting for  $C_0$  in Eqn. (1) and letting  $V_0 = V_\phi - V_R$  one obtains:

$$C(V) = C_m \left( \frac{V_0}{V_\phi - V} \right)^m \quad (3)$$

To obtain the relation between charge and voltage, Eqn. (3) is substituted into the equation:

$$Q = \int C(V) dV$$

to obtain

$$Q = - \frac{C_m V_0^m}{(1-m)} (V_\phi - V)^{1-m} + K$$

When  $V = V_\phi$ , the voltage across the junction is zero, and hence  $Q = 0$ . Therefore  $K = 0$ . So:

$$Q = - \frac{C_m V_0^m}{(1-m)} (V_\phi - V)^{1-m} \quad (4)$$

The charge at voltage  $V_R$  becomes:

$$Q_R = - \frac{C_m V_0^m}{(1-m)} (V_\phi - V_R)^{1-m}$$

The plot of charge versus voltage is given in Fig. (9).

Substituting  $V_0$  for  $V_\phi - V_R$ , the expression for  $Q$  becomes:

$$Q = - \frac{C_m V_0}{(1-m)} \quad (5)$$

Hence Eqn. (4), by use of Eqn. (5), is reduced to:

$$Q = Q_R \left( 1 - \frac{V - V_R}{V_0} \right)^{1-m}$$

which can be rearranged to give:

$$V - V_R = V_0 \left\{ 1 - \left( 1 + \frac{Q - Q_R}{Q_R} \right)^Y \right\} \quad (6)$$

where  $Y = \frac{1}{1-m}$

### Circuit Constraints

Before writing down the circuit equations for Fig. (7), some useful expressions which arise due to the input and output circuit constraints, will be derived. If  $Q_1$  is the instantaneous charge on the varactor at the fundamental frequency due to the input source, then:

$$Q_1 = q_1 \cos \omega t$$

The corresponding fundamental frequency current is:

$$I_1 = i_1 \sin \omega t$$

Similarly, for the output circuit at Nth. harmonic frequency,

$$Q_N = q_N \cos (N\omega t + \phi)$$

and

$I_N = i_N \sin (N\omega t + \phi)$ , where  $\phi$  is the phase angle between the fundamental and the Nth. harmonic currents.

From Fig. (9) it is seen that to obtain the maximum charge swing, the alternating charge components must swing about  $Q_R/2$ . Therefore the net charge,  $Q$ , contained in the diode at any instant is given by:

$$Q = \frac{Q_R}{2} + Q_1 - Q_N.$$



With this value of  $Q$ , Eqn. (6) becomes:

$$V - V_R = V_0 \left\{ 1 - \left( \frac{Q_1 - Q_N + Q_R/2}{Q_R} \right)^x \right\}$$

Substituting for  $Q_1$  and  $Q_N$ , gives

$$V - V_R = V_0 \left[ 1 - \frac{1}{2^x} \left\{ 1 + \frac{q_1 \cos wt}{Q_R/2} - \frac{q_N \cos(Nwt + \phi)}{Q_R/2} \right\}^x \right] \quad (7)$$

As the charge varies periodically, it is possible to expand this expression in a Fourier series. Doing so, Eqn. (7) can be written as:

$$V - V_R = \frac{V_0}{2^x} \left\{ a_0 + \sum_{n=1}^{\infty} (a_n \cos nwt + b_n \sin nwt) \right\} \quad (8)$$

where

$$a_n = -\frac{1}{\pi} \int_{-\pi}^{\pi} \left\{ 1 + \frac{q_1}{Q_R/2} \cos wt - \frac{q_N}{Q_R/2} \cos(Nwt + \phi) \right\}^x \cos nwt \, d(wt) \quad (9)$$

$$b_n = -\frac{1}{\pi} \int_{-\pi}^{\pi} \left\{ 1 + \frac{q_1}{Q_R/2} \cos wt - \frac{q_N}{Q_R/2} \cos(Nwt + \phi) \right\}^x \sin nwt \, d(wt) \quad (10)$$

### Circuit Equations

Having imposed the circuit constraints, one can now proceed to write the mesh equations for the circuit of Fig. (7). For the input circuit:

$$\begin{aligned} E_g \sin(wt + \theta) = i_1 (R_g + R_s) \sin wt + L_1 w i_1 \cos wt \\ + \frac{V_0}{2^x} a_1 \cos wt + \frac{V_0}{2^x} b_1 \sin wt \end{aligned} \quad (11)$$

and for the output

$$\begin{aligned} \frac{V_0}{2^x} a_n \cos Nwt + \frac{V_0}{2^x} b_n \sin Nwt = i_n (R_L + R_s) \sin (Nwt + \phi) \\ + L_N w i_n \cos(Nwt + \phi) \end{aligned} \quad (12)$$

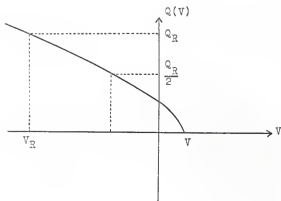


Figure 9. Plot of charge on the varactor versus voltage.

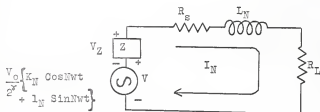


Figure 10. Equivalent output circuit.

Now, in principle, the solution for  $I_N$  in terms of  $E_g$  and the circuit parameters can be found.

It is assumed that the maximum efficiency occurs when the input circuit is resonant at the fundamental frequency and the output circuit is resonant at the  $N$ th. harmonic frequency. Penfield and Rafuse (6) have speculated that some very marginal improvement in efficiency might be possible by detuning either circuit, but this point will not be included in the analysis.

Establishing series resonance in the input circuit results in evaluation of  $L_1$  as follows. From Eqn. (11):

$$L_1 \omega_1 \cos \omega t + \frac{V_0}{2} a_1 \cos \omega t = 0$$

which gives

$$L_1 = - \frac{V_0 a_1}{2 \omega_1} \quad (13)$$

With this value of  $L_1$ , Eqn. (11) becomes:

$$E_g = i_1 (R_g + R_s) + \frac{V_0 b_1}{2} \quad (14)$$

It is not possible to evaluate  $L_N$  in a similar manner, since the phase angle  $\phi$ , of  $I_N$ , is unknown.

In order to find the phase angle  $\phi$ , the output circuit is represented as shown in Fig. (10). That part of  $\frac{V_0}{2} (a_n \cos N\omega t + b_n \sin N\omega t)$  which is independent of  $I_N$  is represented by the generator e.m.f. and the remainder is represented by the voltage across the nonlinear impedance  $Z$ . Thus if the voltage generator is:

$$\frac{V_0}{V} (K_N \cos Nwt + I_N \sin Nwt),$$

then from Eqs. (9) and (10):

$$K_N = -\frac{1}{\pi} \int_{-\pi}^{\pi} \left(1 + \frac{q_1}{Q_R/2} \cos wt\right)^2 \cos Nwt \, d(wt) \quad (15)$$

$$I_N = -\frac{1}{\pi} \int_{-\pi}^{\pi} \left(1 + \frac{q_1}{Q_R/2} \cos wt\right) \sin Nwt \, d(wt) \quad (16)$$

Since  $\left(1 + \frac{q_1}{Q_R/2} \cos wt\right)$  is an even function of  $wt$ ,  $I_N = 0$ .

By adding a term  $\frac{V_0}{2V} K_N \cos Nwt$  to both sides of Eqn. (12) and after some transposition, one obtains,

$$\begin{aligned} \frac{V_0}{2V} K_N \cos Nwt = & -\frac{V_0}{2V} (a_N - K_N) \cos Nwt - \frac{V_0}{2V} b_N \sin Nwt \\ & + L_N N \omega I_N \cos(Nwt + \phi) + I_N (R_L + R_B) \\ & \sin(Nwt + \phi) \end{aligned} \quad (17)$$

Now as  $K_N$  is independent of  $I_N$ , it is required for resonance that  $I_N$  have the same phase as  $\frac{V_0}{2V} K_N \cos Nwt$ . This gives:

$$\begin{aligned} \phi &= \pi/2 \text{ if } K \text{ is positive} \\ &= -\pi/2 \text{ if } K \text{ is negative} \end{aligned}$$

With these values of  $\phi$ , at resonance Eqn. (17) also yields:

$$\pm L_N N \omega I_N = \frac{V_0 b_N}{2} \quad (18)$$

Using these factors, Eqn. (17) becomes:

$$\frac{V_0}{2V} K_N \cos Nwt = -\frac{V_0}{2V} (a_N - K_N) \cos Nwt \pm I_N (R_L + R_B) \cos Nwt$$

which gives

$$i_N = \pm \frac{V_O a_N}{2^v (R_L + R_S)} \quad (19)$$

### Efficiency

The efficiency is defined by the ratio

$$\eta = \frac{\text{Output power}}{\text{Available power from source}}$$

$$\text{Output power} = \frac{i_N^2 R_L}{2}$$

$$\text{Power available from source} = \frac{E_G^2}{8 R_S}$$

Therefore:

$$\eta = \frac{4 i_N^2 R_L R_S}{E_G^2}$$

After substituting the values of  $E_G$  and  $i_N$  from Eqns. (14) and (19) respectively, the above expression becomes:

$$\eta = \frac{4 R_L R_S V_O^2 a_N^2}{2^{2v} (R_L + R_S)^2 \left\{ 1_1 (R_S + R_S) + \frac{V_O b_1}{2^v} \right\}^2} \quad (20)$$

Assuming a specified value of  $1_1$ , the efficiency is optimized with respect to  $R_S$  as follows.

Eqn. (20) can be written as:

$$\eta = \frac{K R_S}{\left\{ 1_1 (R_S + R_S) + \frac{V_O b_1}{2^v} \right\}^2}$$

where

$$K = \frac{4 R_L V_O^2 a_N^2}{2^{2v} (R_L + R_S)^2}$$

Differentiating this with respect to  $R_G$  and equating to zero yields:

$$\bar{R}_G = R_S + \frac{V_0 b_1}{2^{\gamma} I_1} \quad (21)$$

With this value of  $R_G$ , the efficiency becomes:

$$\eta = \frac{V_0^2 a_N^2 R_L}{2^{2\gamma} (R_S + R_G)^2 I_1^2} \quad \frac{1}{R_S + \frac{V_0 b_1}{2^{\gamma} I_1}} \quad (22)$$

In order to have the expression for efficiency in terms of normalized quantities, which is more useful, the following notation is introduced.

$$p_1 = \frac{2q_1}{Q_R} = \frac{2I_1}{Q_R V}$$

$$p_N = \frac{2I_N}{Q_R N V}$$

$$\bar{R}_L = \frac{R_L}{R_S}$$

$$\bar{R}_G = \frac{R_G}{R_S}$$

$$Q_F = \frac{1}{R_S C_m V}$$

Also from Eqn. (5)

$$V_0 = \frac{-(1 - \eta) Q_R}{C_m} = -\frac{Q_R}{\gamma C_m}$$

Substitution of the normalized quantities into Eqn. (22) and simplification yields:

$$\eta = \frac{a_N^2 Q_F^2 \bar{R}_L}{2^{2\gamma-1} p_1 \gamma (1 + \bar{R}_L)^2 (2^{2\gamma-1} p_1 \gamma + Q_F b_1)} \quad (23)$$

Also from Eqn. (19)

$$p_N = \frac{2I_N}{Q_R N V} = \frac{Q_F a_N}{2^{\gamma-1} \gamma N (1 + \bar{R}_L)} \quad (24)$$

The efficiency must be optimized with respect to  $\bar{R}_L$ , however,  $a_N$  and  $b_1$  are functions of  $i_N$ , which in turn is a function of  $\bar{R}_L$ . It would therefore be necessary to differentiate  $a_N$  and  $b_1$  with respect to  $\bar{R}_L$  to optimize the efficiency. This is not analytically possible except in the special case of an abrupt junction. The optimization of efficiency with respect to  $\bar{R}_L$  in the abrupt junction case will now be illustrated.

It was mentioned previously that in the abrupt junction case only the second harmonic is generated, hence  $N$  is equal to 2. Therefore, from Eqn. (9):

$$a_2 = -\frac{1}{\pi} \int_{-\pi}^{\pi} (1 + p_1 \cos wt \pm p_2 \sin 2 wt)^2 \cos 2 wt \delta(wt) dw$$

Upon evaluation, the integral yields

$$a_2 = -\frac{p_1^2}{2}$$

Similarly, from Eqn. (10)

$$\begin{aligned} b_1 &= -\frac{1}{\pi} \int_{-\pi}^{\pi} (1 + p_1 \cos wt \pm p_2 \sin 2 wt)^2 \sin wt \delta(wt) dw \\ &= \mp p_1 p_2 \end{aligned}$$

Substituting for  $p_2$  from Eqn. (24) gives:

$$b_1 = \mp \frac{p_1 Q_F a_2}{8 (1 + \bar{R}_L)}$$

With this value of  $b_1$ , Eqn. (23) becomes:

$$\eta = \frac{a_2^2 Q_F^2 \bar{R}_L}{4 p_1 (1 + \bar{R}_L)} \left\{ 4 p_1 + \frac{Q_F p_1^3 Q_F}{16 (1 + \bar{R}_L)} \right\}$$

which simplifies to:

$$\eta = \frac{p_1^2 Q_p^2 \bar{R}_L}{64 (1 + \bar{R}_L) \left\{ \frac{Q_p^2 p_1^2}{64} + 1 + \bar{R}_L \right\}} \quad (25)$$

To optimize with respect to  $\bar{R}_L$  set  $\frac{d\eta}{d\bar{R}_L} = 0$ .

Doing so, Eqn. (25) yields:

$$\bar{R}_L = 1 + \frac{Q_p^2 p_1^2}{64 (1 + \bar{R}_L)} \quad (26)$$

Also, using  $b_1$  in Eqn. (21) gives:

$$\bar{R}_G = \frac{R_G}{R_S} = 1 + \frac{Q_p^2 p_1^2}{64 (1 + \bar{R}_L)} \quad (27)$$

Equations (26) and (27) show that:

$$\bar{R}_G = \bar{R}_L$$

Also Eqn. (26) can be written as:

$$\bar{R}_L = \sqrt{1 + \frac{Q_p^2 p_1^2}{64}}$$

Substitution of this optimum value of  $\bar{R}_L$  into Eqn. (25) and simplification yields:

$$= \frac{1}{64} \left\{ \frac{p_1^2 Q_p^2}{1 + \left( 1 + \frac{p_1^2 Q_p^2}{64} \right)^{\frac{1}{2}}} \right\}^2 \quad (28)$$

This is the efficiency for a doubler with an abrupt junction varactor. However, if  $\gamma$  is not equal to 2, the general expression for efficiency as given by Eqn. (23) must be evaluated by numerical methods for various values of  $\bar{R}_L$ .



The condition that  $\bar{R}_L$  is equal to  $\bar{R}_G$  is found to hold true always, a fact confirmed by many authors. Therefore in general, for maximum efficiency, it can always be assumed that  $\bar{R}_L = \bar{R}_G = \bar{R}_{in}$ .

#### Limit On Power Output

The limit on efficiency obtained from the varactor, as analyzed above, occurs when the charge swing is so great that forward conduction occurs. At this point:

$$Q = \frac{Q_R}{2} + Q_1 - Q_N = 0$$

Therefore,

$$\frac{d}{d(\omega t)} \left\{ 1 + p_1 \cos \omega t \pm p_N \sin N\omega t \right\} = 0 \quad (30)$$

In order to have the maximum power input into the varactor, the charge must swing about  $Q_R/2$ . Any greater mean charge would, under maximum efficiency conditions, drive the varactor beyond the reverse breakdown limit. Therefore the computations should be carried out within the limit:

$$p_1 \cos \omega t \pm p_N \sin N\omega t \leq 1$$

Figure (11) is the limiting curve of  $p_N$  and  $p_1$  for the doubler with some actual curves of  $p_N$  against  $p_1$  superimposed. Thus knowing the values of  $\gamma$ ,  $Q_r$ ,  $p_1$  and  $N$ , the value of  $p_N$  is known.

#### Design Curves

A set of design curves as computed by Scanlan and Laybourn (7) are given in Figs. (12) to (17); Figs. (12) and (13) show

efficiency versus normalized input power; and curves for  $\bar{R}_{in}$  versus  $p_1$  have been drawn in Figs. (16) and (17). The parameters in all these curves are  $\nu$ ,  $Q_p$  and the order of multiplication. The performance of the varactor can thus be predicted using these design curves.

Example:

Consider a doubler utilizing an abrupt junction varactor with a reverse breakdown voltage  $V_R$  equal to -19 volts and diffusion voltage  $V_\phi$  equal one volt. Other parameters for this diode are:

$$R_s = 1 \text{ ohm} \quad f_c = 4 \times 10^{11} \text{ cps}$$

Let the input frequency be 1 GHz. Now:

$$Q_p = \frac{f_c}{f} = 400$$

Therefore from Fig. (12), curve No. 1, the maximum value of  $p_1$  is 0.7 and the corresponding maximum efficiency is 95 percent. From Fig. (14), curve 1, the normalized input power corresponding to 95 percent efficiency is 105 milliwatts.

The normalization factor is:

$$\frac{V_0^2}{R_s 2^{2\nu+1}} 10^{-5} = \frac{(V_\phi - V_R)}{R_s 2^{2\nu+1}} 10^{-5}$$

For the diode under investigation, the factor becomes:

$$\frac{(20)^2 \times 10^{-5}}{2^5} = 12.5 \times 10^{-5}$$

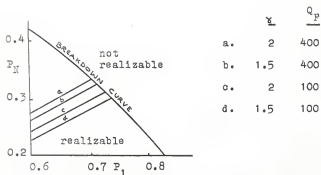
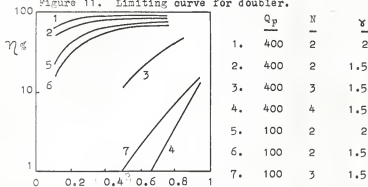
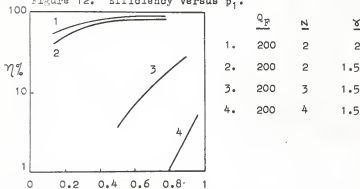


Figure 11. Limiting curve for doubler.

Figure 12. Efficiency versus  $p_1$ .Figure 13. Efficiency versus  $p_1$ .

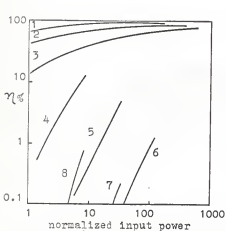


Figure 14. Efficiency versus input power.

	$\gamma$	$\frac{Q_P}{P}$	$N$
1.	2	400	2
2.	2	200	2
3.	2	100	2
4.	1.9	400	3
5.	1.9	200	3
6.	1.9	100	3
7.	1.9	400	4
8.	1.9	200	4

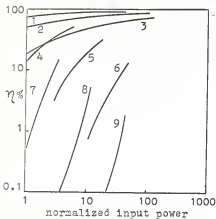
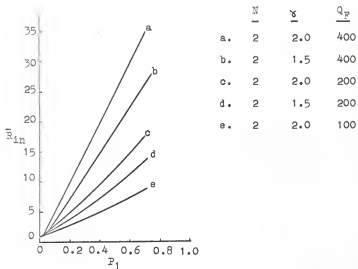
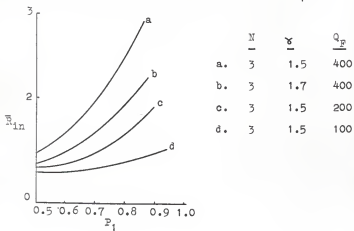


Figure 15. Efficiency versus input power.

	$\gamma$	$\frac{Q_P}{P}$	$N$
1.	1.5	400	2
2.	1.5	200	2
3.	1.5	100	2
4.	1.5	400	3
5.	1.5	200	3
6.	1.5	100	3
7.	1.5	400	4
8.	1.5	200	4
9.	1.5	100	4

Figure 16. Normalized input resistance versus  $P_1$ .Figure 17. Normalized input resistance versus  $P_1$ .

The power output is therefore:

$$P_{\text{out}} = 105 \times 12.5 \times 10^{-5} = 13.12 \text{ mw}$$

The normalized input resistance is found from Fig. (16), curve (a), using  $p_1 = 0.7$

$$\bar{R}_L = \bar{R}_G = \bar{R}_{in} = 36$$

A number of efficiency calculations for different parameter values have been carried out and the results tabulated in Table 1.

Table 1. Results of efficiency of multiplication calculated from the design curves for different varactors and different parameter values.

	N	$V_R$	$V_\phi$	$Q_F$	Max. $p_1$	Max. Efficiency
	2	-19v	1.0v	100	0.7	80%
	1.5	"	"	400	0.85	50%
	1.5	"	"	400	0.95	13%
	2	"	"	400	0.7	95%
	1.5	"	"	400	0.75	90%

#### Observations

The following observations are made regarding the previous results:

- (1) As N increases, the efficiency decreases.

- (2) Figures (12) and (13) show that the efficiency of a doubler is greater for abrupt junction varactor than the graded junction varactor.
- (3) Figures (12) and (13) also show that a high  $Q_F$  is required for good efficiencies. As  $Q_F = f_c/f$ , the cut off frequency,  $f_c$ , should be large and the input frequency relatively low.

Some experimental results show a better efficiency for the graded junction than the abrupt junction varactors. This is because it is possible to build graded junction varactors with a smaller series resistance than the abrupt junction, resulting in a higher value of  $f_c$  and hence of  $Q_F$ . Their comparison is appropriate only if both have the same Q factor, in which case the abrupt junction varactor gives better efficiency.

- (4) The efficiencies obtained in practice will be lower than those predicted for the following reasons:
- (a) The filter and tuning inductances have been assumed ideal.
  - (b) The diode itself has been somewhat idealized.
  - (c) The spreading resistance of the semiconductor material varies with applied voltage, because the width of the depletion layer varies, changing the thickness of the remaining semiconductor.
  - (d) Any stray capacitance tends to lower the efficiency, because of shunting effects.

It should be kept in mind that the analysis assumes a diode voltage variation from  $V_R$  to  $V_\phi$ . In practice this range can be exceeded to obtain a larger value of  $p_1$  and greater efficiency. However, such operation is apt to produce noise, which might be undesirable (6).

In summary, for good efficiency and large power output, the varactor selected should have:

- (1) High Q factor
- (2) Large breakdown voltage
- (3) Small series resistance



## ANALYSIS WITH IDLERS

A varactor multiplier with idler circuits is analyzed in this section. The method of solution is similar to the one without idlers, and follows the procedure adopted by Scanlan and Laybourn (8).

The equivalent circuit of the multiplier is shown in Fig. (18) where, for generality more than one idler circuit is assumed. The filters are such that filter  $F_k$  allows current to flow only at the  $k$ th. harmonic. The general idler frequency is denoted as  $m$ th. harmonic, and the output frequency is denoted as the  $N$ th. harmonic.

The charge on the varactor at the fundamental frequency is:

$$Q_1 = q_1 \cos \omega t$$

and the charge at the  $k$ th. harmonic is:

$$Q_k = q_k \cos(k\omega t + \phi_k)$$

The corresponding  $k$ th. harmonic current is:

$$I_k = i_k \sin(k\omega t + \phi_k)$$

where  $\phi_k$  is the phase difference between the fundamental and the  $k$ th. harmonic currents.

For the maximum charge swing:

$$Q = Q_D + Q_1 - \sum Q_k$$

where  $Q_D$  is the mean charge on the diode.

Therefore, with the addition of idlers, Eqn. (7) becomes:

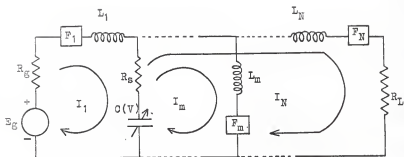


Figure 18. The equivalent circuit of a varactor harmonic multiplier with idlers.

$$V - V_R = V_0 \left[ 1 - \frac{1}{2^{\gamma}} \left( \frac{Q_D}{Q_R/2} + \frac{q_1 \cos \omega t}{Q_R/2} - \sum \frac{q_k \cos(k\omega t + \phi_k)}{Q_R/2} \right)^{\gamma} \right] \quad (31)$$

The summation is taken over all harmonic currents which are allowed to flow, including the output frequency.

Expanding Eqn. (31) as a Fourier series yields:

$$V - V_R = \frac{V_0}{2^{\gamma}} \left[ a_0 + \sum_{n=1}^{\infty} (a_n \cos n\omega t + b_n \sin n\omega t) \right]$$

where

$$a_n = -\frac{1}{\pi} \int_{-\pi}^{\pi} \left( \frac{Q_D}{Q_R/2} + \frac{q_1 \cos \omega t}{Q_R/2} - \sum \frac{q_k \cos(k\omega t + \phi_k)}{Q_R/2} \right)^{\gamma} \cos n\omega t d(\omega t) \quad (32)$$

$$b_n = -\frac{1}{\pi} \int_{-\pi}^{\pi} \left( \frac{Q_D}{Q_R/2} + \frac{q_1 \cos \omega t}{Q_R/2} - \sum \frac{q_k \cos(k\omega t + \phi_k)}{Q_R/2} \right)^{\gamma} \sin n\omega t d(\omega t) \quad (33)$$

### Circuit Equations

The equations for the input and output circuits are the same as Eqns. (11) and (12) with  $\phi$  now replaced by  $\phi_{in}$ . For maximum efficiency, the equation for the input circuit is the same as Eqn. (14), that is,

$$E_g = I_1 (R_g + R_e) + \frac{V_0 b_1}{2^{\gamma}} \quad (34)$$

At each idler frequency the equation is:

$$\frac{V_0}{2\gamma} (a_m \cos m\omega t + b_m \sin m\omega t) = i_m R_g \sin(m\omega t + \phi_m) + i_m L_m \cos(m\omega t + \phi_m) \quad (35)$$

After introducing normalizations as before and with the notation

$$R_g = \frac{2^{\gamma} R_g}{V_0}$$

$$Q_R = -\frac{C_m V_0}{1-m} = -C_m V_0 \gamma$$

$$P_N = \frac{2i_N}{Q_R N W}$$

$$i_N = -N W Q_N$$

and

$$Q_F = \frac{1}{R_S C_m W}$$

equation (34) becomes:

$$\bar{R}_g = p_1 \gamma \frac{2^{\gamma-1}}{Q_F} \left[ \bar{R}_g + 1 + \frac{b_1 Q_F}{\gamma 2^{\gamma-1} p_1} \right] \quad (36)$$

In this equation, since  $\bar{R}_g$  is the normalized generator resistance, the remainder of the term in the brackets is recognized as the normalized (non-linear) input impedance at the particular drive level. Therefore for maximum power transfer:

$$\bar{R}_g = \left( 1 + \frac{Q_F b_1}{\gamma 2^{\gamma-1} p_1} \right) \quad (37)$$

With this, Eqn. (36) becomes:

$$\bar{E}_G = \frac{\gamma 2^\gamma}{Q_F} p_1 \left( 1 + \frac{Q_F b_1}{\gamma 2^{\gamma-1} p_1} \right) \quad (38)$$

Equation (12), after normalization becomes:

$$\frac{1}{\gamma 2^{\gamma-1}} (a_N \cos N\omega t + b_N \sin N\omega t) = \frac{N p_N}{Q_F} (1 + \bar{R}_L) \sin(N\omega t + \phi_N) + \frac{L_N N^2 \omega p_N}{Q_F R_S} \cos(N\omega t + \phi_N) \quad (39)$$

Similarly, Eqn. (35) reduces to:

$$\frac{1}{\gamma 2^{\gamma-1}} (a_m \cos m\omega t + b_m \sin m\omega t) = \frac{m p_m}{Q_F} \sin(m\omega t + \phi_m) + \frac{L_m m^2 \omega}{Q_F R_S} p_m \cos(m\omega t + \phi_m) \quad (40)$$

Upon expanding the right hand side of Eqn. (40) and solving for  $p_m$  and  $L_m$ , the following two equations are obtained:

$$p_m = \frac{Q_F}{m \gamma 2^{\gamma-1}} (a_m \sin \phi_m + b_m \cos \phi_m) \quad (41)$$

$$\frac{L_m m \omega}{R_S} = \frac{Q_F}{m \gamma 2^{\gamma-1} p_m} (a_m \cos \phi_m - b_m \sin \phi_m) \quad (42)$$

Equation (41) is helpful in the calculation of efficiency and Eqn. (42) is useful for determining the inductance values.

### Efficiency

The general expression for efficiency is:

$$\eta = \frac{4 I_N^2 R_L R_G}{E_G^2}$$

For matched input:

$$E_G = 2I_1 R_G$$

Therefore:

$$\begin{aligned} \eta &= \frac{I_N^2 R_L}{I_1^2 R_G} \\ &= \frac{N^2 P_N^2 \bar{R}_L}{P_1^2 \bar{R}_G} \end{aligned}$$

If  $m = N$ , Eqn. (41) becomes

$$P_N = \frac{Q_F}{N\gamma^2} (a_N \sin\phi_N + b_N \cos\phi_N)$$

With this value of  $P_N$  and with the expression for  $\bar{R}_G$  from Eqn. (37), the efficiency becomes:

$$\eta = \frac{\left(\frac{Q_F}{\gamma^2}\right)^2 (a_N \sin\phi_N + b_N \cos\phi_N)^2 \bar{R}_L}{P_1^2 \left(1 + \frac{Q_F b_1}{\gamma^2 p_1}\right)} \quad (43)$$

### Breakdown Curve

The limits on the instantaneous charge are:

$$0 \leq Q(t) \leq Q_R$$

That is,

$$0 \leq Q_D + q_1 \cos wt - \sum q_m \cos (mwt + \phi_m) \leq Q_R$$

With the normalization:

$$p_0 = \frac{Q_D}{Q_R/2}$$

$$p_1 = \frac{q_1}{Q_R/2}$$

$$p_m = \frac{q_m}{Q_R/2}$$

the limits become:

$$2 \gg p_0 + p_1 \cos \omega t - \sum p_m \cos (m\omega t + \phi_m) \gg 0 \quad (44)$$

In principle, any circuit can be analyzed using Eqs. (32), (33), (38), (39) and (40). However in practice this process is extremely difficult, even using numerical techniques. The fact that maximum efficiency and power output are obtained by operating on the breakdown curve, as given by Eqn. (44), can be used in the analysis and leads to some simplification.

#### Resonance Considerations

The output and the idler circuits are represented in a manner similar to the representation of the output circuit shown in Fig. (10). The diode voltage is taken to be composed of two parts, one a function of  $p_n$  and the other independent of it. The values of  $K_n$  and  $l_n$  are obtained by setting the appropriate  $p_n$  equal to zero in Eqs. (32) and (33); and the other coefficients are then found using the condition  $p_n$  equal to zero. Even this process, except for the abrupt junction case, is difficult.

#### Specific Cases

Consider the case of an abrupt junction varactor used as a tripler, operating with an idler at the second harmonic. Thus:

$$m = 2 \quad N = 3$$

The first step is to evaluate  $K_2$  and  $l_2$ . Setting  $p_2 = 0$  also implies  $p_3 = 0$ , since the abrupt junction varactor is only capable of generating the second harmonic in absence of idlers.

Thus, from Eqn. (32)

$$K_2 = -\frac{1}{\pi} \int_{-\pi}^{\pi} (p_0 + p_1 \cos wt)^2 \cos 2wt \, d(wt)$$

$$= -\frac{p_1^2}{2}$$

and from Eqn. (33)

$$I_2 = -\frac{1}{\pi} \int_{-\pi}^{\pi} (p_0 + p_1 \cos wt)^2 \sin 2wt \, d(wt) = 0$$

This is a development similar to the one which lead to Eqns. (15) and (16). Therefore adopting a similar procedure leads to Eqn. (17), which gives:

$$\phi_2 = \pm \pi/2$$

Next  $K_3$  and  $I_3$  are evaluated as follows:

$$K_3 = -\frac{1}{\pi} \int_{-\pi}^{\pi} \left\{ p_0 + p_1 \cos wt - \bar{p}_2 \cos (2wt \pm \pi/2) \right\}^2 \cos 3wt \, d(wt)$$

$$I_3 = -\frac{1}{\pi} \int_{-\pi}^{\pi} \left\{ p_0 + p_1 \cos wt - \bar{p}_2 \cos (2wt \pm \pi/2) \right\}^2 \sin 3wt \, d(wt)$$

$$= + p_1 \bar{p}_2$$

where  $\bar{p}_2$  is the value of  $p_2$  in the absence of third harmonic output.

Using these values to evaluate  $\phi_3$  from Eqn. (12) results in

$$\phi_3 = 0, \pi.$$

If the abrupt junction varactor is used as a quadrupler with an idler at the second harmonic, then the solution yields:

$$\phi_4 = \pm \pi/2$$

The above values for the phase angles were for an abrupt



junction varactor. For a graded junction varactor they are difficult to evaluate. However, in general, it is assumed that the phase angles for the graded junction are the same as for the corresponding abrupt junction case.

#### Method Of Solution

As the angles found above result in a symmetric charge waveform, for maximum efficiency and power output,  $p_0$  is chosen to be unity. The equation for the breakdown curve and Eqn. (41) are used at a particular value of  $p_1$  to obtain  $p_N$ . Equation (39) is then used to obtain the corresponding value of  $\bar{R}_L$ , and  $\bar{R}_G$  is obtained from Eqn. (37). With this information, the efficiency is determined. This procedure is repeated for other values of  $p_1$ .

#### Design Curves

Computational results obtained by Scanlan and Laybourn (8) are shown in Figs. (19) to (28). Figure (19) shows a typical set of breakdown curves. Figures (20) and (21) show the variation of efficiency versus  $p_1$ , with  $Q_F$  as a parameter. The curves are for an abrupt junction tripler and quadrupler with an idler at the second harmonic. Figure (22) shows the relative efficiencies for the abrupt and graded junction triplers with idlers, and Fig. (23) compares the power output for the two types of varactors. Figures (26) and (27) have been plotted similarly for quadruplers. The variation of load and input resistances versus input frequency for different values of  $\gamma$  is shown in Figs. (24) and (25).

A plot of efficiency versus frequency for a quadrupler is shown in Fig. (28). Curves for three different ways of achieving the fourth harmonic are shown; that is, without idlers, with idlers and with cascaded doublers. The figure, in effect, contains the essence of this section.

### Conclusions

Comparison of efficiencies obtained with and without idlers clearly indicates the advantages obtained by including idler circuits. For example in case of a graded junction tripler for a  $Q_p$  value of 100, the maximum efficiency obtainable with idler is 55 percent and without idler is 15 percent. The power output is also greater with the idler. These results can be explained on a physical basis as follows. The efficiency of conversion to the second harmonic from Fig. (12) is 80 percent and to the third harmonic without idlers is 15 percent. With an idler at the second harmonic, mixing with the fundamental results in more of the third harmonic. So an increase in both efficiency and power output is obtained, as both the multiplying and mixing processes have been utilized to advantage.

The efficiencies and power outputs for triplers, and quadruplers with an idler at second harmonic are greater for an abrupt junction varactor than with a graded junction varactor. This is because the coupling between the fundamental and the second harmonic is greatest for the abrupt junction varactor.

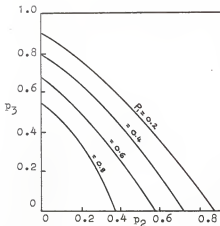


Figure 19. Breakdown curves for a tripler with idler at second harmonic.

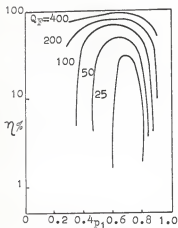


Figure 20. Abrupt junction tripler with second harmonic idler.

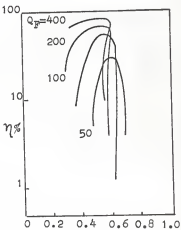


Figure 21. Abrupt junction quadrupler with second harmonic idler.

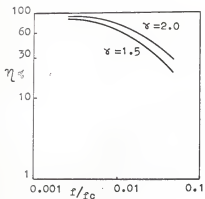


Figure 22. Max. efficiency as a function of normalized frequency for a tripler.

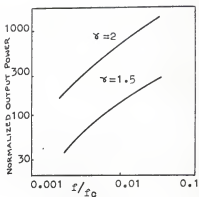


Figure 23. Max. output power as a function of normalized frequency for a tripler.

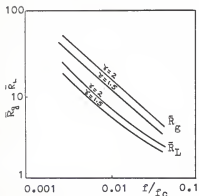


Figure 24. Load and input resistances to produce max. efficiency in a tripler.

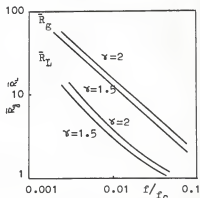


Figure 25. Load and input resistances to produce max. efficiency in a quadrupler.

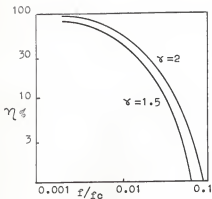


Figure 26. Max. efficiency as a function of normalized freq. for a quadrupler.

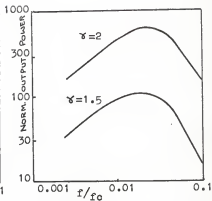


Figure 27. Max. output power as a function of normalized freq. for a quadrupler.

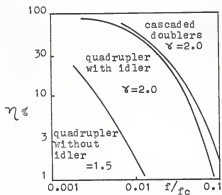


Figure 28. Comparison of efficiencies obtained with a quadrupled output.

Figure (28) shows a comparison of efficiencies obtained for a quadrupler by cascading two doublers and by using an idler at the second harmonic. It is observed that the efficiencies achieved by these two methods are nearly the same.

From the above results, the use of idlers seems to be an attractive means of achieving better efficiency and power output. But it should be noted that this is obtained at the expense of increased circuit complexity. Therefore, the idlers are avoided where the efficiency is not of prime importance, or where other means of achieving better efficiency are available. One such way is by hyperabrupt varactors, which forms the subject of investigation in the next section.

### THE HYPERABRUPT VARACTOR MULTIPLIER

A hyperabrupt diode is a semiconductor diode with a large value of  $m$ , the nonlinearity coefficient. At first the dependence of efficiency on the nonlinearity coefficient is shown, which suggests the use of hyperabrupt varactors for high order multiplication. Thus good high order multiplication efficiencies are obtained without the use of idlers.

#### Efficiency And The Nonlinearity Coefficient

Before proceeding with the analysis, the dependence of efficiency on the nonlinearity coefficient will be demonstrated mathematically. Equation (3) is expressed as an elastance (reciprocal capacitance) voltage relationship by:

$$S(V) = S_m \left( \frac{V_\phi + V}{V_\phi + V_R} \right)^m \quad (45)$$

where  $S_m$  is the elastance at the breakdown voltage, and  $V$ , the applied voltage, is now taken opposite in sign to that of Eqn. (3). Figure (29) shows the plot of  $\frac{S}{S_m}$  versus

$$\frac{V_\phi + V}{V_\phi + V_R} .$$

Now,

$$S = \frac{1}{C} = \frac{dV}{dQ} \quad (46)$$

By combining Eqns. (45) and (46) one obtains:

$$dQ = \frac{(V_\phi + V_R)^m}{S_m} \frac{dV}{(V_\phi + V)^m} \quad (47)$$

Integration yields:

$$Q = \frac{(V_\phi + V_R)^m}{(1-m)S_m} (V_\phi + V)^{1-m} + K_1 \quad (48)$$

for  $m$  not equal to unity. When  $V$  is equal to  $-V_\phi$ , the charge on the junction is zero, hence  $K_1$  is zero. Therefore:

$$Q = \frac{(V_\phi + V_R)^m}{(1-m)S_m} (V_\phi + V)^{1-m} \quad (49)$$

The maximum charge,  $Q_m$ , that the junction can support is at the breakdown voltage,  $V_R$ . Therefore, at  $V$  equal to  $V_R$  Eqn. (49) becomes:

$$Q_R = \frac{V_\phi + V_R}{(1-m)S_m} \quad (50)$$

Equation (49) in terms of  $Q_R$  becomes:

$$Q = Q_R \left[ \frac{V_\phi + V}{V_\phi + V_R} \right]^{1-m} \quad (51)$$

Which is rewritten in the form:

$$\frac{V_\phi + V}{V_\phi + V_R} = \left( \frac{Q}{Q_R} \right)^{\frac{1}{1-m}} \quad (52)$$

Figure (30) is a plot of normalized voltage as a function of normalized charge. As  $m$  approaches zero, the voltage charge curve approaches a straight line and the diode capacitance becomes constant. As  $m$  increases from zero towards unity, the capacitance deviates more severely from linearity. It is seen from Eqn. (50) that  $Q_R$  is a function of  $m$ . Thus the maximum charge the junction can support increases as  $m$



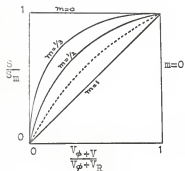


Figure 29. Normalized elastance as a function of normalized voltage.

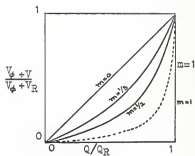
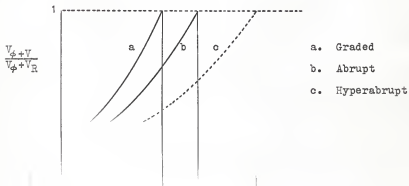


Figure 30. Normalized voltage as a function of normalized charge.



increases. Therefore it should be noted that the normalizing factor of charge,  $Q_R$ , in Fig. (30) is a function of  $m$ . By substituting the appropriate value of  $m$  into Eqn. (50) one obtains:

$$(Q_R)_{A.J.} = \frac{2 (V_\phi + V_R)}{S_m} \quad (53)$$

for the abrupt junction and,

$$(Q_R)_{G.J.} = \frac{3}{2} \frac{(V_\phi + V_R)}{S_m} \quad (54)$$

for graded junction.

The normalized diode voltage  $\frac{(V_\phi + V)}{V_\phi + V_R}$  plotted as a function of normalized charge for the abrupt junction is shown in Fig. (31). Curves for the graded and hyperabrupt varactors are also shown.

The instantaneous power is the product of voltage and current, and current is the time derivative of charge. From Fig. (31) it is seen that for any value of  $V$ , the value of  $Q$  is greatest for the hyperabrupt varactor. Hence the current and therefore the power must be greater for greater value of  $m$ . This suggests the use of hyperabrupt varactors for high order multipliers.

#### The Multiplier Analysis

Design curves for large values of  $m$  were not computed in the previous analysis of a varactor multiplier without idlers hence the performance of a hyperabrupt varactor cannot be predicted by use of Figs. (12) to (15). Therefore the

analysis here is carried out from the beginning. A slightly different procedure, as outlined by Markand and Yuan (5) is adopted, with some changes in notation. However it is in conformity with the notation introduced earlier in this section. As before, the analysis is at first carried out in general terms and after a certain stage a specific example is taken up to simplify the mathematics involved.

The total charge  $Q$  is written as:

$$Q = q_0 + q \quad (55)$$

where  $q_0$  is the charge at the quiescent point, and  $q$  is the time varying component. Expansion about the quiescent point yields:

$$\begin{aligned} f(Q) &= f(q_0 + q) \\ &= f(q_0) + f'(q_0)q + \frac{f''(q_0)q^2}{2} + \dots \\ &\quad + \frac{1}{n} f^n(q_0)q^n + \dots \end{aligned} \quad (56)$$

where  $f^n(q_0)$  is the  $n$ th. derivative evaluated at the bias point. From Eqns. (50) and (51):

$$\begin{aligned} V + V_\phi &= S_m(1-m) \frac{Q}{(Q_R)^{\frac{m}{1-m}}} \\ &= f(Q) \end{aligned} \quad (57)$$

By expanding in Taylor's series and evaluating at  $q_0 = \frac{Q_R}{2}$  one obtains:

$$\begin{aligned}
 V + V_{\phi} = & \frac{Q_R}{2(\Gamma + 1)} S_0 + S_0 q + \frac{\Gamma}{Q_R} S_0 q^2 + \frac{4\Gamma(\Gamma-1)}{6Q_R} S_0 q^3 \\
 & + \dots + \frac{2^{n-1}}{n!} \frac{\Gamma!}{(\Gamma-n+1)!(Q_R)^{n-1}} S_0 q^n + \dots \quad (58)
 \end{aligned}$$

where  $\Gamma = \frac{m}{1-m}$

and

$$S_0 = f^1(q_0) = \frac{S_m}{2^n} \quad (59)$$

If currents only at the input angular frequency  $\omega$  and the output angular frequency  $N\omega$  are allowed to flow, then the current flowing through the diode is:

$$\begin{aligned}
 i(t) &= i_1(t) + i_N(t) \\
 &= I_1 \cos(\omega t + \theta) + I_N \cos(N\omega t + \phi) \quad (60)
 \end{aligned}$$

In general  $V_{\phi}$  is much smaller than the applied voltage  $V$ . Therefore, including the effects of the spreading resistance  $R_s$ , the diode terminal voltage,  $V_T(t)$ , becomes from Eqn. (58):

$$\begin{aligned}
 V_T(t) = & \frac{Q_R}{2(1+\Gamma)} S_0 + R_s i(t) + S_0 \left[ \int i(t) dt \right] + \frac{\Gamma}{Q_R} S_0 \left[ \int i(t) dt \right]^2 \\
 & + \dots + \frac{2^{n-1}}{n!} \frac{\Gamma!}{(\Gamma-n+1)!(Q_R)^{n-1}} S_0 \left[ \int i(t) dt \right]^n + \dots \quad (61)
 \end{aligned}$$

### General Procedure

All equations derived up to Eqn. (61) are exact and general, and the general procedure for solution is as follows:

(1) Substitute Eqn. (60) in Eqn. (61).

- (ii) Extract the coefficients of all terms involving the angular frequencies  $w$  and  $Nw$  for the voltage across the varactor terminals at the respective frequencies.
- (iii) Add the external circuit and derive the matrix equation that describes the operation of the circuit.
- (iv) Derive the equation for efficiency as a function of the load resistance and drive level.
- (v) Optimize the efficiency.

#### Specific Example

A particular case of a hyperabrupt varactor, with  $m$  equal to 0.75, used as quadrupler, is now considered.

The current flowing through the diode is:

$$i(t) = I_1 \cos(\omega t + \theta) + I_4 \cos(4\omega t + \phi) \quad (62)$$

and the charge is:

$$q = \frac{I_1}{\omega} \sin(\omega t + \theta) + \frac{I_4}{4} \sin(4\omega t + \phi). \quad (63)$$

$$\text{Let } U = I_1 \sin(\omega t + \theta) + \frac{I_4}{4} \sin(4\omega t + \phi).$$

Then substitution of Eqns. (62) and (63) into (61) yields:

$$\begin{aligned} V_T(t) = & \frac{Q_R}{2(1+\Gamma)} S_0 + R_S \left[ I_1 \cos(\omega t + \theta) + I_4 \cos(4\omega t + \phi) \right. \\ & + \frac{S_0}{\omega} U + \frac{\Gamma}{\omega Q_R} \frac{S_0}{\omega} U^2 + \dots \\ & \left. + \frac{2^{n-1}}{n!} \frac{\Gamma!}{(\Gamma-n+1)!} [\omega Q_R]^{n-1} \frac{S_0}{\omega} U^n + \dots \right] \quad (64) \end{aligned}$$

For  $m = 0.75$ ,  $\Gamma = 3$ . Therefore Eqn. (64) terminates at  $n$  equal to 4, in the series:

$$\begin{aligned}
 V_T(t) &= \frac{Q_R}{U} S_0 + R_S \left[ I_1 \cos(\omega t + \theta) + I_4 \cos(4\omega t + \phi) \right. \\
 &+ \frac{S_0}{W} U + \frac{3}{WQ_R} \frac{S_0}{W} U^2 + \frac{4}{[WQ_R]^2} \frac{S_0}{W} U^3 \\
 &+ \left. \frac{2}{WQ_R} \frac{S_0}{W} U^4 \right] \quad (65)
 \end{aligned}$$

#### External Circuit Constraints

Circuit constraints similar to those shown in Fig. (8) are now introduced. For this specified circuit, the performance is determined by evaluating the varactor terminal voltages at frequencies  $\omega$  and  $4\omega$ . These voltages are evaluated by collecting the coefficients at each frequency from Eqn. (65). Thus the procedure is to expand the  $U$  terms, express the trigonometric powers in terms of the multiple angles, and then collect the appropriate terms. Doing so, the voltage,  $V_1(t)$  for the fundamental is:

$$\begin{aligned}
 V_1(t) &= R_S I_1 \cos(\omega t + \theta) + \frac{S_0}{W} I_1 \sin(\omega t + \theta) \\
 &+ I_1 \sin(\omega t + \theta) \left\{ \frac{3}{4} I_1^2 + \frac{3}{2} \left( \frac{I_4}{4} \right)^2 \right\} \frac{4}{[WQ_R]^2} \frac{S_0}{W} \\
 &- I_1^3 \left( \frac{I_4}{4} \right) \frac{\cos(\omega t + \phi - 3\theta)}{2} \frac{2}{WQ_R} \frac{S_0}{W} \quad (66)
 \end{aligned}$$

Similarly, the voltage,  $V_4(t)$ , for the fourth harmonic is:

$$\begin{aligned}
 V_4(t) &= R_S I_4 \cos(4\omega t + \phi) + \frac{S_0}{\omega} \frac{I_4}{4} \sin(4\omega t + \phi) \\
 &+ \left(\frac{I_4}{4}\right) \sin(4\omega t + \phi) \left\{ \frac{3}{2} I_1^2 + \frac{3}{4} \left(\frac{I_4}{4}\right)^2 \right\} \left[ \frac{4}{\omega Q_R} \right]^2 \frac{S_0}{\omega} \\
 &+ \frac{I_1}{4} \frac{\cos(4\omega t + 4\theta)}{2} \left[ \frac{2}{\omega Q_R} \right]^3 \frac{S_0}{\omega}
 \end{aligned} \tag{67}$$

If the generator voltage in Fig. (8) is taken as  $E_G \cos(\omega t + \theta)$ , then at resonance, the mesh equations, using cosine phasors, become:

$$E_G e^{j\theta} = (R_G + R_S) I_1 e^{j\theta} - \frac{I_1}{\omega Q_R} \left(\frac{I_4}{4}\right) e^{-j3\theta} e^{j\phi} \tag{68}$$

$$0 = \frac{I_1^4}{4} e^{j4\theta} \left[ \frac{1}{\omega Q_R} \right]^3 \frac{S_0}{\omega} + (R_S + R_L) I_4 e^{j\phi} \tag{69}$$

By use of the notation:

$$e_G = E_G e^{j\theta} \tag{70}$$

$$i_1 = I_1 e^{j\theta} \tag{70}$$

$$i_4 = I_4 e^{j\phi} \tag{71}$$

$$M_1 = \frac{I_1}{\omega Q_R} e^{j\theta} = m_1 e^{j\theta} \tag{72}$$

$$M_1^* = \frac{I_1}{\omega Q_R} e^{-j\theta} = m_1 e^{-j\theta} \tag{73}$$

the mesh equations are written in the matrix form:

$$\begin{aligned}
 \begin{bmatrix} e_g \\ 0 \end{bmatrix} &= \begin{bmatrix} R_g + R_s & -\frac{M_1^3}{4} \frac{S_0}{W} \\ \frac{M_1^3}{4} \frac{S_0}{W} & R_s + R_L \end{bmatrix} \begin{bmatrix} i_1 \\ i_4 \end{bmatrix} \\
 &= \begin{bmatrix} R_{t1} & -B \\ 0 & R_{t2} \end{bmatrix} \begin{bmatrix} i_1 \\ i_4 \end{bmatrix}
 \end{aligned} \tag{74}$$

Where

$$\begin{aligned}
 R_{t1} &= R_g + R_s \\
 R_{t2} &= R_L + R_s
 \end{aligned} \tag{75}$$

and

$$\begin{aligned}
 B &= \frac{M_1^3}{4} \frac{S_0}{W} \\
 0 &= \frac{M_1^3}{4} \frac{S_0}{W}
 \end{aligned} \tag{76}$$

Solving Eqn. (74) for  $i_1$  and  $i_4$  gives:

$$i_1 = e_g \frac{R_{t2}}{R_{t1} R_{t2} + B0} \tag{77}$$

$$i_4 = e_g \frac{-0}{R_{t1} R_{t2} + B0} \tag{78}$$

Dividing Eqn. (78) by Eqn. (77) gives the phase-angle relationship:

$$i_4 = i_1 - \frac{0}{R_{t2}} \tag{79}$$



$$I_4 e^{j\phi} = -I_1 e^{j\theta} \frac{m_1}{4R_{t2}} \frac{e^{j3\theta} S_0}{W} \quad (80)$$

Thus:

$$\phi = 4\theta + \pi$$

and

$$I_4 = I_1 \frac{m_1^3}{4R_{t2}} \frac{S_0}{W} \quad (81)$$

The equivalent circuit at the fundamental frequency is shown in Fig. (32). The input impedance is:

$$\begin{aligned} Z_{in} &= \frac{e}{I_1} - R_G = R_{t1} + \frac{BC}{R_{t2}} - R_G \\ &= R_0 + R_S \end{aligned} \quad (82)$$

where

$$R_0 = \frac{BC}{R_{t2}} = \frac{m_1^6}{16} \left( \frac{S_0}{W} \right)^2 \frac{1}{R_{t2}} \quad (83)$$

Physically,  $R_0$  is the equivalent conversion resistance, since it is the resistance reflected into the input loop by the load resistance.

#### Efficiency

The power delivered to the load is:

$$P_L = \frac{I_4^2 R_L}{2} \quad (84)$$

and the power available from the generator is:

$$P_{AV} = \frac{3g}{8R_G}$$

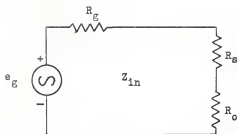


Figure 32. Equivalent circuit at the fundamental frequency.

Therefore, the efficiency becomes:

$$\eta = \frac{I_h^2 4R_L R_G}{E_G^2}$$

$$= \frac{G^2}{(R_{t1} R_{t2} + BC)^2} 4R_L R_G$$

By substituting for some of the expressions previously defined and manipulating, one obtains:

$$= \frac{4R_G R_O (R_S + R_O)}{(R_G + R_S + R_O)^2} \frac{1}{(R_S + R_O)} \frac{R_L}{R_{t2}}$$

For matched input

$$R_G = R_O + R_S$$

Therefore:

$$\eta = \frac{1}{1 + \frac{R_S}{R_O}} \frac{1}{1 + \frac{R_S}{R_L}} \quad (85)$$

### Optimization

Having obtained the expression for efficiency, the parameters are optimized as follows: First, the equation describing the operation over the full range is derived. This helps in choosing a suitable value of  $m_1$ . Next, the efficiency is optimized with respect to  $R_L$ . Lastly, the optimum bias voltage is determined.

For convenience, Eqn. (57) is rewritten as:

$$V + V_\phi = S_m (1-m) \frac{G}{R} \frac{1-m}{1-m^2}$$

When the full range of the varactor is utilized,  $\frac{C_0 C}{C_0 + C}$  reaches a maximum value of unity during each cycle of the periodic diode voltage. Since:

$$S = \frac{dV}{dQ} = S_M \left( \frac{Q}{Q_M} \right)^{\frac{m}{1-m}}$$

at the maximum value:

$$\frac{S}{S_M} = 1 = \left( \frac{Q}{Q_M} \right)^{\frac{m}{1-m}} = \left( \frac{Q}{Q_M} \right)^3$$

where  $Q_M$  is the maximum value of  $Q$ . Therefore:

$$\frac{Q}{Q_M} = 1 \tag{86}$$

Now:

$$Q_M = q_0 + q_m$$

where  $q_0$  is equal to  $Q_R/2$  and  $q_m$  is the value of  $q$  when  $Q$  is equal to  $Q_M$ . With this, Eqn. (86) becomes

$$\frac{1}{2} + \frac{q_m}{Q_R} = 1$$

The value of  $q_m$  at instant  $t_1$  is substituted from Eqn. (63), with  $\phi$  equal to  $4\theta$ , to yield:

$$1 = \frac{1}{2} + m_1 \sin(\omega_1 t + \theta) + m_4 \sin(4\omega_1 t + 4\theta) \tag{87}$$

where

$$m_1 = \frac{I_1}{\omega Q_R}$$

and

$$m_4 = -\frac{I_4}{4\omega Q_R}$$

Equation (87) is the equation which describes the operation over the whole range. Penfield and Rafuse (6) have shown that when the varactor is fully driven, the value of  $m_1$  attains a maximum value of  $1/2$ . This in effect describes the maximum current that can flow at the fundamental frequency, as:

$$I_1 = wQ_R m_1$$

The optimum value of  $R_L$  is found by setting

$$\frac{d\eta}{dR_L} = 0$$

and solving for  $R_L$ . This yields:

$$R_L = \sqrt{K + R_S^2} \quad (88)$$

where

$$K = \frac{m_1^6}{16} \left( \frac{S_0}{W} \right)^2 \quad (89)$$

The optimum bias voltage is obtained by setting

$$Q_B = q_0 = \frac{Q_R}{2}$$

in Eqn. (49). Here  $Q_B$  is the charge at the bias voltage.

Therefore:

$$\frac{Q_R}{2} = \frac{(V_\phi + V_R)^m}{(1-m)S_m} (V_\phi + V_0)^{1-m}$$

In this equation,  $V_0$  is the applied dc bias voltage. Solving for  $V_0$ , one obtains:

$$V_0 = \left[ \frac{Q_R}{2} \frac{(1-m)S_m}{(V_\phi + V_R)^m} \right]^{\frac{1}{1-m}} - V_\phi \quad (90)$$

The value of  $Q_R$  is determined from Eqn. (50).

### Results

Consider the example of a quadrupler with the following numerical values.

$$S_0 = \frac{1}{1 \times 10^{-12}} \text{ (farads)}^{-1}$$

$$R_s = 1 \text{ ohm.}$$

$$\text{Input frequency} = 2 \times 10^{10} \text{ radians per sec.}$$

$$\omega_c = 2\pi f_c = 1 \times 10^8 \text{ radians per sec.}$$

$$m_1 = 1/2$$

This value of  $m_1$  gives maximum efficiency, as mentioned previously.

With these values:

$$K = \left(\frac{1}{2^6}\right) \frac{1}{16} \left(\frac{1}{2 \times 10^{-12}}\right)^2 = 2.45$$

$$R_L = \sqrt{2.45 + 1^2} = 1.86$$

$$R_{t2} = R_s + R = 2.86$$

$$R_0 = \frac{m_1^6}{16} \left(\frac{S_0}{\omega}\right)^2 \frac{1}{R_{t2}}$$

$$= \frac{K}{R_{t2}} = \frac{2.45}{1.86} = 1.32$$

Therefore:

$$\eta = \frac{1}{1 + \frac{R_s}{R_0}} \frac{1}{1 + \frac{R_s}{R_L}}$$

$$= \frac{1}{1 + \frac{1}{1.32}} \frac{1}{1 + \frac{1}{1.86}}$$

which gives:

$$= 37\%$$

#### Efficiency Versus Drive Level

It is clear from the efficiency relation that in order to obtain a higher value of efficiency, a higher optimum value of  $R_L$  is required. This in turn requires greater value of  $K$  and hence  $m_1$ . The maximum achievable value of  $m_1$  for any varactor is  $1/2$ , if the range of operation is  $V_R$  to  $V_\phi$  (Penfield and Rafuse 6). However, if  $V_\phi$  is exceeded, it results in a greater value of  $m_1$ , hence greater efficiency. Thus as the drive level goes up, so does the efficiency.

The use of hyperabrupt varactors becomes even more attractive when much higher harmonics are required. Efficiency as high as 55% is predicted by Markand and Yuan (5) for an eight times multiplier for  $m = 0.875$ , and as high as 81% if the diode has  $m = 0.92$ .

To summarize, the use of hyperabrupt varactor has the following advantages:

1. High efficiency for high order multiplication without idlers.

2. Ease of tuning due to the simplicity of the circuit, since only an input frequency loop and an output frequency loop are required.
3. Higher power handling capability as compared to abrupt varactors, with the same breakdown voltages.

At the present time, when varactor junctions are made hyperabrupt, it is done at the expense of cut off frequency. However, as  $m$  increases, there is a net increase in the conversion resistance,  $R_0$ , in spite of the effect of the degraded cut off frequency. Hence, for low order multipliers, hyperabrupt varactors have no particular advantage over the ordinary ones, however they do offer definite advantages when used for high order multiplication.



## CONCLUSIONS

The analysis of the varactor harmonic generator reveals that the efficiency increases with increase in drive level and with increase in nonlinearity coefficient of the diode, while the efficiency decreases with increasing input frequency. For low order multiplication, say 2 or 3, an ordinary diode can be used, but for higher orders the efficiency falls off rapidly.

The abrupt junction diode is incapable of generating harmonics other than the second, therefore, with such diodes the use of idlers is necessary to obtain higher harmonics. Even with other diodes the introduction of idlers is always seen to improve the efficiency and power output. The use of hyperabrupt varactors also improves the efficiency considerably, and thus provide an alternate means to get high order multiplication.

Results for efficiency obtained for a quadrupler by three different methods with about the same values of parameters at  $f/f_c$  equal to 0.02 are as follows:

By use of idlers	30%
By cascading two doublers	33%
By hyperabrupt varactor	37%

Of the three methods, the use of hyperabrupt varactor seems to be the better one, not only because of the higher efficiency, but also because of the simplicity of circuitry and tuning involved. A high Q factor and large breakdown voltage are required of any varactor for better efficiency.

## ACKNOWLEDGMENT

The author wishes to express his deep appreciation, to his major advisor Dr. N. R. Malik, for his guidance, suggestions and discussions at various stages of the work.

## BIBLIOGRAPHY

1. Ghausi, S. G., "Principles and Design of Linear Active Circuits". McGraw Hill Book Company, 1965.
2. Johnson, K. M., "Large Signal Analysis of Parametric Harmonic Generators". IRE Transactions on Microwave Theory and Techniques, September 1960, 8:525.
3. Leeson, D. B. and S. Weinreb, "Frequency Multiplication with Nonlinear Capacitors-A Circuit Analysis". Proc. IRE., December 1959, 47(12):2076.
4. Manley, J. M. and H. E. Rowe, "Some General Properties of Nonlinear Elements. Part 1 General Energy Relations". Proc. IRE., July 1956, 44(7):904.
5. Markand, E. and S. Yuan, "High Efficiency, High Order, Idlerless Frequency Multipliers Using Hyperabrupt Varactors". RCA Review, September 1965, 26(3):400.
6. Penfield, P. and R. P. Rafuse, "Varactor Applications". MIT Press, 1962.
7. Scanlan, J. O. and P. J. R. Laybourn, "Large Signal Analysis of Varactor Harmonic Generators Without Idlers". Proc. IEE., August 1965, 112(8):1515.
8. Scanlan, J. O. and P. J. R. Laybourn, "Large Signal Analysis of Varactor Harmonic Generators With Idlers". The Radio and Electronic Engineer., June 1966, 31(6).
9. Utsunomiya, T. and S. Yuan, "Theory, Design and Performance of Maximum Efficiency Variable Reactance Frequency Multiplier". Proc. IRE., January 1962, 50:57.

LARGE SIGNAL OPERATION OF VARACTOR MULTIPLIERS

by

VAJINDER PAL SINGH

B. S., (Hons. School) Physics, Panjab University, India 1962

M. S., (Hons. School) Physics, Panjab University, India 1963

---

AN ABSTRACT OF A MASTER'S REPORT

submitted in partial fulfillment of the

requirements for the degree

MASTER OF SCIENCE

Department of Electrical Engineering

KANSAS STATE UNIVERSITY

Manhattan, Kansas

1967

## ABSTRACT

Varactor harmonic generators are being increasingly used to obtain power in the microwave region. The essential features of such a device are low series resistance, low noise and simplicity. It is the objective of this report to theoretically investigate the performance of varactor multipliers from a large signal point of view.

In order to use the varactor advantageously an insight to the physical concepts is at first given. This leads to an intuitive understanding of the behavior of a varactor and yields limits on its operation.

The analysis has been developed both with and without idlers. It is observed that the inclusion of idlers always adds to the performance of the varactors, though it is done at the expense of circuit complexity.

For better efficiency, diodes with a high  $Q$  and large breakdown voltage and large nonlinearity coefficient are desirable. The hyperabrupt varactor which makes use of the last property, and thus avoids idlers, is also analyzed.

Three different ways of generating harmonics are discussed; quadrupler with idlers, and by using a hyperabrupt varactor. The results obtained by these three methods show almost identical performances.